Atmos. Chem. Phys. Discuss., 12, 18959–18991, 2012
www.atmos-chem-phys-discuss.net/12/18959/2012/
doi:10.5194/acpd-12-18959-2012

Atmospheric Chemistry and Physics Discussions

Future Antarctic ozone recovery rates in September–December predicted by CCMVal-2 model simulations

J. M. Siddaway[1], **S. V. Petelina**[1], **D. Karoly**[2], **A. R. Klekociuk**[3], and **R. J. Dargaville**[2]

[1]Department of Physics, La Trobe University, Bundoora VIC 3086, Australia
[2]School of Earth Sciences, University of Melbourne, Melbourne VIC 3010, Australia
[3]CPC Program, Australian Antarctic Division, Kingston TAS 7050, Australia

Received: 15 June 2012 – Accepted: 10 July 2012 – Published: 1 August 2012

Correspondence to: J. M. Siddaway (j.siddaway@latrobe.edu.au)

Published by Copernicus Publications on behalf of the European Geosciences Union.

Abstract

Chemistry-climate model validation phase 2 (CCMVal-2) model simulations are used to analyze Antarctic ozone recovery rates in 2000–2100 during local spring and early summer, both vertically integrated and at several pressure levels in the lower stratosphere. Multi-model median trends of monthly zonal mean total ozone column (TOC), ozone volume mixing ratio (VMR), wind speed and temperature poleward of 60° S are investigated. Median values are used to account for large variability in models, and the associated uncertainty is calculated using a bootstrapping technique. According to the selected ten CCMVal-2 models, Antarctic TOC will return to its pre-ozone hole level, taken as an average of 1970–1979 values, between 2065 and 2075 in September–November, and around 2050 in December. In 2000–2020, an increase in TOC is much smaller than in later years, and this is especially evident for December. Although the December TOC recovers to its pre-ozone hole levels earlier compared to all spring months (as the December ozone depletion was much lower), the rate of December TOC increase, is slower than that for all spring months. Projected trends in ozone VMR, temperature and winds at several pressure levels are analyzed in order to attribute the projected rate of December TOC recovery, as well as to investigate future changes in the Antarctic atmosphere in general, including some aspects of the polar vortex breakup.

1 Introduction

It has been over 25 yr since the first measurements of significant stratospheric ozone depletion over Antarctica (Farman et al., 1985) was linked with an increase in anthropogenic halogen loading (e.g. Solomon et al., 1986). That discovery led to the establishment of the Montreal Protocol in 1987 to regulate global emissions of ozone depleting substances (ODS), such as chlorofluorocarbons (CFCs), containing Cl_y and Br_y compounds. A peak in surface ODS emissions was observed in mid-1990s, and these emissions are now in decline (WMO, 2007). Such decline is often measured by equivalent effective stratospheric chlorine (EESC) levels. EESC combines Cl_y and Br_y into a single quantity that leads to ozone depletion. Following on from the decline in surface emissions, global mean concentrations of EESC, also peaked in late 1990's, are now decreasing as well (e.g. Newman et al., 2007). Successful outcomes of global agreements, such as the Montreal Protocol, provide an indication that regulations of anthropogenic emissions entering the atmosphere are achievable and beneficial.

Establishing when the ozone layer over Antarctica begun to recover and how long the recovery to pre-ozone hole levels might take is important, as this information may inform future policy on halogen compound production. The subject of when the ozone recovers and at what rates has many other important implications, such as possible effects of this process on surface climate in Antarctica (Perlwitz et al., 2008) and over the Southern Hemisphere in general (Son et al., 2010). Antarctic ozone recovery also affects lower stratospheric circulation and mean age of air in the Northern Hemisphere (Deushi and Shibata, 2011). Zeng et al. (2010) found that with recovery of stratospheric ozone over the 21st century, a significant increase in extra-tropical tropospheric ozone is expected. Specifically, stratosphere-troposphere exchange (STE) processes will lead to a 4–8 ppbv increase in surface ozone in the Southern Hemisphere winter months, which has significant ramifications for air quality. Importantly for polar marine ecology, ozone depletion has resulted in increased levels of high latitude erythermal solar irradiance (UV-Ery). With the ozone recovery, the UV-Ery levels will continue to change rapidly and are expected to return to their 1980 levels by 2050 (Bais et al., 2011).

The most accurate presently available method to investigate how a reduction in atmospheric halogen loading to natural "background" levels will lead to stratospheric ozone recovery in the near future is to analyse simulations from state-of-the-art coupled chemistry-climate models (CCMs). Such models are widely used to predict the future behavior of stratospheric ozone in response to different forcings (e.g Eyring et al., 2007). They provide simulations of various atmospheric parameters in three-dimensional space coupled with fully interactive stratospheric ozone chemistry. The

ACPD
12, 18959–18991, 2012

degree of ozone recovery can also be moderated by other changes in the atmospheric composition, such as current and future increase in concentrations of greenhouse gases (GHG). These will affect ozone levels and complicate the attribution of direct ozone recovery from decreased halogens (Eyring et al., 2010b). Possible GHG effects are also accounted for in the latest CCM simulations.

The aim of this study is to analyze Antarctic ozone recovery with respect to historical baseline of 1970–1979 values using the output from several CCMs. This is considered an indirect ozone recovery, as the direct ozone recovery is defined as the date when ozone is no longer under the influence of anthropogenically produced ODS. As a result, return of stratospheric ozone to a certain pre-defined value and a full ozone recovery can be reached at different times (Waugh et al., 2009; Eyring et al., 2010a). We examine zonally averaged values of ozone volume mixing ratio and total ozone column poleward of 60° S for the months of September–December. We also analyze effects of a projected ozone recovery on the polar vortex by assessing temperature and zonal mean zonal wind variations over the September–December period.

2 Model description

Stratospheric processes and their role in climate project (SPARC) chemistry-climate model validation phase 2 (CCMVal-2) report (SPARC CCMVal, 2010) is a coordinated model intercomparison that included results from up to 17 CCMS, with some models providing a wider variety of simulations than others. 16 of these models offer future reference simulations (REF-B2) for the SPARC CCMVal-2 activity to project ozone trends towards the end of the 21st century (Eyring et al., 2010a). REF-B2 simulations are transient simulations from 1960 to 2100 that contain time series of surface hydrocarbon halogens based on the adjusted World Meteorological Organisation (WMO) A1 scenario (WMO, 2007) and surface GHG concentrations based on the special report on emissions scenario A1B (IPCC, 2000). These REF-B2 simulations of the future atmospheric state essentially include anthropogenic forcings only, such as varying GHG

ACPD
12, 18959–18991, 2012

surface concentrations and prescribed halogen emissions, with natural forcings due to solar variability and volcanic activity being excluded. Even though these model simulations begin in 1960, anthropogenic forcings based on observations are not included for the "past" period. This is different from REF-B1 simulations that include both natural and anthropogenic forcings (Eyring et al., 2007). Combining both REF-B1 and REF-B2 model simulations, however, is not considered in this study, as it is preferential to work with a continuous and homogenous dataset. A quasi-biennial oscillation (QBO) signal is only included in those models that internally simulate QBO, namely MRI and UM-SLIMCAT (Eyring et al., 2007). All models except one (CMAM) have prescribed sea surface temperature (SST) and sea ice cover (SIC) from coupled ocean model simulations (Eyring et al., 2010a; Morgenstern et al., 2010). A more detailed description of each model formulation is given by SPARC CCMVAL (2010) and by Morgenstern et al. (2010) and will not be repeated here.

Monthly mean total ozone column (TOC) values were available for 13 models that participated in the REF-B2 simulations. Three out of these 13 models had to be excluded from the present analysis: GEOSCCM had a discontinuous future simulations commencing in 2000, UMUKCA-METO only provided data until 2083, and CAM3.5 output was considered an outlier as its ozone fields deviated from those of other models by 100 %, or more. Previous diagnostics for CAM3.5 in relation to natural ozone variability also reported that it was an outlier (Austin et al., 2010), possibly due to a lower atmospheric ceiling compared to other models (SPARC CCMVAL, 2010). There were variations in the ensemble size for each model: most models provided a single ensemble member, with the exception of MRI (2 ensemble members) and the CMAM, SOCOL, ULAQ and WACCM models (3 ensemble members). For each model with more than one ensemble member, the mean value of them was taken.

ACPD
12, 18959–18991, 2012

3 Data Analysis and Discussion

3.1 Methodology

To investigate the projected evolution of the Antarctic ozone, simulated monthly mean TOC data were zonally averaged poleward of 60° S. We considered the months of September–December, when the Antarctic stratospheric ozone depletion has mainly been observed in the past, and analyzed variations of ozone with respect to corresponding pre-ozone hole baseline level. This baseline level is an averaged value of TOC that has not yet been significantly perturbed by ODS. There are differing opinions on what year to select as a baseline for ozone recovery estimations. It is common to use the 1980 value (e.g WMO, 2007), which is an average of 1975–1984 values, as the ozone depletion in the Antarctic vortex was relatively small at that time. On the other hand, Newman et al. (2007) reported that EESC have been increasing rapidly before 1985, and thus the 1975–1984 baseline period may not represent the unperturbed ozone period. In this work, a baseline derived from a mean of 1970–1979 values of ozone and temperature is used, hereafter referred to as a 1975 baseline. This 1975 baseline represents relatively unperturbed levels of stratospheric ozone not yet significantly affected by anthropogenic halogen emissions (e.g. Farman et al., 1985).

While many studies that analyze the ozone hole metric employ multi-model mean TOC values, here we use multi-model median TOC and ozone volume ratio (VMR) values. As the spread in individual model outputs can be large, especially for ozone concentrations at various pressure levels, using the median function gives an advantage of assigning a lower weight to the most deviating model simulations. To quantify the uncertainty associated with the multi-model median values, namely a 95 % confidence level, a bootstrapping technique was used. In order to generate the statistical uncertainty, a subsample of individual model median values was randomly sampled with replacement 1000 times to produce a normal distribution of medians. From this distribution, a confidence limit was calculated.

Figure 1 shows the time series of TOC for individual CCMVal-2 model outputs for the months of September–December over the period of 1960–2100. The names of all 10 models used in this study are indicated on the bottom right panel. While there is significant variation in TOC between each model output, nearly all models suggest a minimum TOC value around the year 2000 for all months. The multi-model median value and the 95 % confidence limit of the median derived using a bootstrapping method is also shown in Fig. 1. Red stars indicate corresponding observational data, which are zonally averaged monthly mean TOC values measured by the Total Ozone Mapping Spectrometer (TOMS), merged ozone dataset (MOD) (e.g. Stolarski and Frith, 2006) version 8.5, in 1979–2011. It can be seen that the 95 % confidence interval of the multi-model medians and the TOMS data agree well. While some individual model TOC outputs show good agreement with observations, other models produce either too high, or too low TOC values. However, this bias is not consistent for all months considered. As the individual model intercomparison and validation is not part of this work, we did not exclude any model based on their agreement with the TOMS TOC in Fig. 1. Part of the reason for this is the fact that some models could be in good agreement with the measured TOC, but not in a good agreement in relation to winds or temperature. Nevertheless, we repeated all steps of the presented below analysis for only those 4 models that show a very good agreement with TOMS TOC for each month considered in this study. These four models are clearly identifiable on the bottom right Panel of Fig. 1. We found that such narrow selection of models did not significantly change main results and conclusions of this work, including return dates of TOC to 1975 baseline value and recovery rates (both as a percentage value of monthly baseline values, and as an increase in DU per decade). This could be, in part, due to the fact that the bootstrapping statistical analysis technique employed here minimizes the effect of individual outliers when multi-model median is calculated. It is also worth reminding that interannual variability in TOMS data results from variability associated with combined natural and anthropogenic forcings, while CCMVal-2 models consider anthropogenic forcing only. European Centre for Medium-Range Weather Forecasts (ECMWF) ERA-interim reanalysis data (Dee et al., 2011) in 1979–2010 were also compared with CCMVal-2 TOC values in Fig. 1 (not shown) and, similar to TOMS data, were within the 95 % confidence limit for models. We also note that CCMVal-2 models used here have a range of grid resolutions (e.g Morgenstern et al., 2010) that could possibly introduce a weighting bias when calculating an all-model trend. In order to investigate this further, time series of ozone mass poleward of 60° S were produced. These results (not shown here) suggest that differences in model grid resolutions do not affect the analysis presented in this work.

3.2 Trends in total ozone column

Multi-model monthly zonal median of TOC deviation from the 1975 baseline for the period of 1960–2100, both a percentage and an absolute deviation, are shown in Figs. 2 and 3, respectively. The data are smoothed with a 15-yr uniformly weighted sliding mean filter, and vertical dash-dotted lines indicate the year when TOC returns to its baseline value for each month. The percentage values shown in Fig. 2 are median percentage deviations relative to the 1975 baseline for that month. Percentage values of ozone VMR and temperature, which will be discussed later, are also calculated in the same way. Figures 2 and 3 suggest that September–November and December TOC return to their pre-ozone hole levels between 2065–2075 and by approximately 2050, respectively. In Fig. 3, median absolute deviations are shown by dashed lines, and the grey shaded area represents the 95 % confidence level of the multi-model medians. This confidence level shows an uncertainty, often asymmetric, in the return date to the 1975 baseline in the order of ±20 to ±30 yr, with October and November having an upper uncertainty limit beyond 2100.

As seen in Fig. 3, the highest ozone depletion of ~ 110 DU relative to the 1975 baseline occurs in October. This is about 30 DU larger than the ozone depletion relative to the 1980 baseline in REF-B2 simulations (e.g. Eyring et al., 2010a). Figure 3 also shows that a minimum TOC value for all months is between 2000 and 2005. Assuming that the ozone hole is defined as a region where TOC value is less than 220 DU (e.g.

ACPD
12, 18959–18991, 2012

Newman et al., 2004), we found that its size, calculated from CCMVal-2 model outputs (not shown here), has reached its maximum also between 2000 and 2005.

Figures 2 and 3 suggest that in 2000–2050, the rate of TOC recovery in December is somewhat slower than that for spring months, even though the December TOC recovery to the 1975 baseline value occurs earlier. This effect is quantified in Tables 1 and 2 that show monthly decadal TOC recovery rates, both as a percentage of the corresponding 1975 baseline value, and in DU $decade^{-1}$, respectively. Note that after about 2050, the December TOC is fully recovered and continues to increase as stratospheric halogen levels decrease further under the REF-B2 scenario (in both tables, recovery rates for decades where TOC exceeds the baseline values are italicized). TOC recovery rates are at their peak are 2030–2039 for September and 2020–2029 for October–December. Also, the decadal rate of TOC increase in December are generally lower than those for all other months, and this is particularly evident in 2000–2019.

Salby et al. (2011) found that a statistically significant positive trend in TOC during the ozone hole season is not expected in the first few decades of the 21st century. CCMVal-2 model simulations suggest that this is true for November and December, at the end of the Antarctic ozone hole season, but not expected during the season's peak in September and October. Using a parametric model and a future ODS scenario similar to that employed in the REF-B2 model runs, Newman et al. (2006) found that the ozone hole area decreased by $\sim 0.3\,\%\,yr^{-1}$ until 2010. In comparison, we found that the CCMVal-2 multi-model median of ozone hole area, averaged over September–October (not shown), decreased by $\sim 0.6\,\%\,yr^{-1}$ in 2000–2010.

3.3 Trends in Ozone VMR at various stratospheric altitudes

To analyse patterns in TOC recovery over Antarctica within the stratosphere, we produced vertical profiles for deviations of ozone VMR from baseline (Fig. 4). Similar to previous plots, model data have been smoothed with a 15-yr uniformly weighted sliding mean filter. Ozone VMR are plotted for all available pressure levels considered by CCMVal-2 models in the range of 20–150 hPa. This range covers the region where the majority of atmospheric ozone over Antarctica is located and where most of the depletion takes place (e.g. Solomon et al., 2005). All left panels in Fig. 4 show percent deviations from baseline and all right panels show median ozone VMR values. Dotted lines on right panels indicate the multi-model uncertainty range, which increases with increasing altitude for all months. Figure 4 shows that in September, the SH percentage (absolute) polar ozone loss is greatest at 50 (30) hPa, in October – at 70 (50) hPa, and in November and December – at 100 (70) hPa. Thus, the region of the largest ozone loss moves from higher altitudes in early spring to lower altitudes in early summer. This result is supported by observations of chemical tracers, which show that in spring, air transport within the Antarctic stratosphere is directed downwards (Solomon, 1999). It is also supported by one of the conclusions in SPARC CCMVal (2010) that by early summer, the breakdown of the polar vortex and the strengthening Brewer-Dobson circulation cause the descent of ozone-rich air from high polar altitudes to the lower stratosphere. A recent observational example of this effect – time series of zonally averaged vertical ozone profiles poleward of 60° S in 2002–2009, were reported in Klekociuk et al. (2011) in their Fig. 14a. In that example, the upper edge of the ozone hole descends from ∼ 19 km in early October to ∼15 km in early December.

Based on 25 yr of ozonesonde measurements at the South Pole and the Georg-Forster/Neumayer Antarctic stations, Hassler et al. (2011) investigated minimum daily ozone VMR at 50 hPa in late September to early October. Their data, as a vertical profile of percent ozone loss for 5 yr averages between day 235 and 270 (see their Fig. 5c) indicate that the loss rates increased at 150–50 hPa, but decreased at 40–20 hPa. CCMVal-2 model projections for the same months show the maximum ozone loss occurring between 70 and 50 hPa, which agrees well with measurements of Hassler et al. (2011).

At 150 hPa, the deviation of ozone VMR from baseline is smallest, and a return to baseline occurs in ∼ 2055 for all months. At 100–70 hPa, ozone VMR does not fully recover to its 1975 values for spring months, and after ∼ 2070, these values are no longer increasing. The December ozone at these altitudes almost recovers to baseline

ACPD
12, 18959–18991, 2012

values in ∼2070, which is about 20 yr later than the December TOC recovery date. At 50 hPa, the September and October ozone VMR recover to 1975 baseline around 2070–2080, but November and December ozone VMR do not fully recover.

As the pressure decreases (altitude increases), the December, and to a lesser extent November, ozone shows less depletion. At 30 hPa, the December ozone is not significantly depleted – its VMR deviates from the baseline by less than 0.2 ppmv (about 5 % of the baseline value). At 20 hPa, the December ozone VMR remains above the baseline, and the November ozone VMR is lower than the baseline by less than 0.3 ppmv (also about 5 % of the baseline value). These are the likely reasons for the observed delay in December TOC recovery during 2010–2050 shown in Figs. 2 and 3, and also for slower rates of recovery for November and December TOC given in Tables 1 and 2. These results can be linked to the fact that by early summer, the breakdown of the polar vortex and strengthening Brewer–Dobson circulation bring descending ozone-rich air to the polar lower stratosphere (SPARC CCMVAL, 2010).

3.4 Trends in stratospheric temperatures and winds

In order to better understand projected Antarctic ozone recovery trends and their relation to other atmospheric parameters, we also investigate trends in stratospheric temperature and winds. These parameters, also provided by CCMVal-2 model simulations, relate to changes in the size and strength of the polar vortex as halogen concentrations decrease (e.g. Waugh and Polvani, 2010). Monthly zonal mean fields for these metrics were obtained at same pressure levels as ozone VMR in Fig. 4. Zonal mean temperatures were calculated poleward of 60° S, whereas zonal mean zonal wind speeds were averaged over the 50°–70° S range. This range covers latitudes where the edge of the polar vortex is expected to be throughout the 21st century.

Time series for monthly zonal mean REF-B2 temperatures are plotted in Fig. 5, where left panels show percent deviations and right panels show absolute deviations from the 1975 baseline. Figure 5 suggests a general decrease in the lower stratospheric temperatures until 2000, when ozone was decreasing as well. A comparison

ACPD
12, 18959–18991, 2012

of Figs. 4 and 5 suggest a correlation between lower temperatures and lower ozone levels. Such a correlation is likely to arise from temperature-dependent polar stratospheric chemistry, including ODS reactions and horizontal and vertical transport of air caused by planetary waves (e.g. Wirth, 1993; Solomon et al., 2005). At 150–100 hPa, CCMVal-2 multi-model temperatures return to baseline by the end of the 21st century for all months. But at, and above, altitudes corresponding to 70 hPa, stratospheric temperatures do not recover to their 1975 baseline values, which can be attributed to the projected increase in GHG concentrations as stated in the A1B scenario (IPCC, 2000). CCMVal-2 models suggest that during the ozone depletion period of 1975–2000, temperature trends at 100 hPa were –0.5 to –1.5 K $decade^{-1}$ for September–October months, and ~2 K $decade^{-1}$ for November–December months. Randel et al. (2009) analyzed satellite, radiosonde and lidar temperature observations in 1979–2007 at 100 hPa over the same latitude range and found a similar cooling trend of about –1 K $decade^{-1}$ for spring months and –1.5 K $decade^{-1}$ for summer months. The period of the maximum temperature deviation from baseline in Fig. 5 generally coincides with the period of maximum depletion in ozone VMR observed in Fig. 4. December temperatures have the largest deviation from baseline at 100 hPa, November – at 70 hPa, October – at 50 hPa, and September – at 20 hPa. These deviations in temperature correlate with deviations in ozone at the same pressure levels for most months. September temperature is at its minimum at the end of the 21st century rather than during the peak ozone depletion around the year ~2000. December temperature also shows slower recovery at 50–70 hPa, in agreement with the slower December TOC recovery.

At 30 hPa, December temperatures show no significant trend during the period of ozone depletion and until ~2000. At altitudes above 30 hPa, an initial increase in December temperature is followed by its decrease towards the end of the 21st century. For this period, December ozone VMR in Fig. 4 shows a small decrease and then an increase at higher pressure levels. Both December ozone and December temperature time series indicate a reversal in the radiative effect of ozone. In the lowermost

ACPD
12, 18959–18991, 2012

stratosphere, ozone and temperature correlate: a decrease in ozone levels leads to a decrease in temperature. But at higher altitudes they anti-correlate: an increase in ozone is associated with a radiative cooling observed from ~2000 for all months. This anti-correlation is seen at 20 hPa for all months and also down to 30 hPa for December. As will be discussed later, such a decrease in temperature could be related to CO_2-induced cooling, which in turn leads to a slowdown in ozone destruction reactions (e.g. Shepherd and Jonsson, 2008).

During the recovery period of 2000–2050, December lower stratospheric temperatures are influenced by the ozone recovery with warming occurring at altitudes up to 50 hPa. Above these heights, stratospheric cooling increases with increasing altitude, with no temperature recovery to 1975 baseline due to effects of long-term CO_2 cooling. If the lower stratosphere cooling associated with ozone depletion could lead to a strengthening of the polar vortex, then warming associated with ozone recovery would decrease the stability of the vortex and affect future persistence of the vortex into early summer. To analyze this effect, monthly zonal mean zonal winds are plotted in Fig. 6 at same pressure levels as temperatures in Fig. 5 and ozone VMR in Fig. 4. Waugh et al. (1999) found that similar to potential vorticity (PV), zonal wind is a useful diagnostics in assessing the breakup of the polar vortex, although not as highly derivative. As noted earlier, we consider wind data averaged across 50°–70° S, which encompasses the location of the edge of the polar vortex (e.g. Lee et al., 2001). Wind speeds across smaller 5° latitude bins were also analyzed in this work (not shown), and the resulting trends were similar to those for the 50°–70° S region.

The dot-dashed lines at the 15 $m s^{-1}$ level in Fig. 6 indicate the minimum wind speed, below which the vortex is considered to have broken up (Nash et al., 1996). For all pressure levels analysed, spring month winds indicate that the polar vortex is present over the entire time period. For December, model outputs suggest that at heights above 50 hPa, the polar vortex is broken-up. However, at altitudes below 50 hPa, the December wind speed of $\geq 15\ m s^{-1}$ indicates that the vortex edge is present until the middle of the 21st century. As the polar vortex collapses in early summer, its edge could either disappear, or first shift poleward, and then disappear. To analyze whether the December zonal mean wind speed exceeded the $15\,\mathrm{m\,s^{-1}}$ limit at higher latitudes compared to what is shown in Fig. 6, monthly zonal wind data were also considered at higher latitudes of 70°–80° S. These results (not shown) showed trends in zonal wind speeds at each pressure level very similar to those in Fig. 6, suggesting that stratospheric polar vortex quickly collapses in December.

Figure 6 indicates that increasing polar westerlies, associated with ozone depletion, are seen in the lower stratosphere during November and December until ~2000. During the ozone recovery period, there is a corresponding decrease in polar westerlies. When compared with results for TOC and ozone VMR in Figs. 2, 3 and 4, there is about a one month time lag in zonal wind response to changes in ozone VMR. Overall, there is no significant trend in zonal winds for the months of September–October. Monier and Weare (2011) found similar results with the ECMWF ERA-40 reanalysis data over the time period of 1980–2001, with a strengthening westerly wind associated with ozone depletion via the thermal wind balance.

Zonal winds were also considered with respect to trends seen in the monthly TOC values. The 1975 baseline wind value $\bar{U}_{\mathrm{base}}$ and a mean peak value $\bar{U}_{\mathrm{peak}}$ between 2000–2005 are used to produce the time series for normalized zonal wind percentage deviation, $\%U_{\mathrm{dev}}$, as shown in Fig. 7. This normalized wind percentage deviation of annual wind speed values $U(t)$ is calculated as:

$$\%U_{\mathrm{dev}} = \left(\frac{U(t) - \bar{U}_{\mathrm{base}}}{\bar{U}_{\mathrm{peak}} - \bar{U}_{\mathrm{base}}} \right) \times 100\,\% \tag{1}$$

As September wind data had high absolute wind values but small variability, in order to be shown together with other months they were scaled by a factor of 100 (divided by 100) for 150 and 100 hPa and by a factor of 10 for other altitudes.

Figure 7 suggests that the percent increase in zonal wind speed during the ozone depletion period is very similar between all months. However, when compared to October and November, the December winds indicate a delay in the rate of recovery of

ACPD
12, 18959–18991, 2012

relative zonal wind speed to baseline until approximately 2050. Starting from 100 hPa, this effect increases with increasing height. Thus, lower December TOC recovery rates in 2010–2050 and slower December wind speeds in 2010–2050 could be related. By 2100, model projections indicate a net increase in wind speeds for all months, compared to the 1975 baseline values, due to an indirect effect of increasing surface GHG concentrations via temperature changes. The increasing effect of GHG is also seen in the secondary peak in zonal wind median at all pressure levels for all months except September.

There is evidence that austral summer wind speeds increase significantly, both in the troposphere and in the stratosphere, due to decreasing ozone and increasing GHG concentrations (Thompson and Solomon, 2002; Shindall and Schmidt, 2004; Perlwitz et al., 2008; Son et al., 2010). According to these studies, future changes in SH atmospheric circulation due to ozone recovery are expected to be opposed by increases in tropospheric GHG. However, effects from increasing ozone concentrations and decreasing ozone hole size will still dominate at Antarctic latitudes until 2100.

4 Concluding remarks

In this work, ten CCMVal-2 model simulations are used to analyze Antarctic ozone recovery in 2000–2100 during September–December. Multi-model median values of monthly zonal mean TOC, ozone VMR, wind speed, and temperature poleward of 60° S are used. Uncertainty associated with multi-model medians is calculated using a bootstrapping technique. It is found that September–November TOC will return to corresponding 1975 baseline values between 2065 and 2075 (±25 yr), while December TOC will return to its pre-ozone hole level around 2050 (−20 + 30 yr). We also note that this analysis of ozone recovery is based on zonal averages, and thus the previously reported zonal asymmetries in the TOC field (e.g. Grytsai et al., 2007) may lead to some local variations in ozone recovery dates.

ACPD
12, 18959–18991, 2012

Antarctic TOC recovery rates are found to vary for different months and decades throughout the 21st century. In 2000–2020, TOC recovery rates are quite low for all months, and in December they are significantly, at times by more than a factor of 10, lower compared to some other months. In 2020–2030, TOC decadal recovery rates are similar for all months, but in 2030–2059, those for December are again noticeably lower. Model simulations suggest that in early spring, the maximum contribution to decrease in TOC comes from ozone depletion at higher altitudes, and in early summer – from ozone depletion at lower altitudes. This is in agreement with various independent observations discussed in Sect. 3.3.

At 100–50 hPa, the December ozone returns to the 1975 baseline 25 yr later than the December TOC for reasons that are not yet clear. It can only be speculated whether lower stratospheric ozone is influenced by continuously increasing GHG or continuously decreasing halogen levels, as REF-B2 model simulations combine the effects from these anthropogenic forcings. Newman et al. (2006) found that full ozone recovery to 1980 levels, based purely on future ODS levels, will occur around 2068. Together with results from this study, this would suggest removal of anthropogenic ODS by ~2070, and that any subsequent changes in polar ozone would be due to increasing GHG. Alternatively, Waugh et al. (2009) found that when the effect of climate change alone was considered, there were minimal decadal-scale variations in polar ozone during the 21st century. In that study, mean October ozone VMR at 50 hPa, as well as October TOC, were predicted to recover to 1960 values by 2100, due to the combined forcing effect of GHG and ODS.

The effects of future ozone recovery on stratospheric temperatures and winds were also considered in this study. Multi-model median trends in monthly temperatures correlate well with ozone within the lower stratosphere – as expected with temperature-dependent polar stratospheric chemistry, where temperatures rise with ozone recovery. However, at altitudes corresponding to 20–30 hPa, there is a reversed radiative effect due to a combined effect of increased GHG and decreased ODS concentrations. At altitudes above ~10 hPa, stratospheric cooling can lead to a decreased efficiency of

ACPD
12, 18959–18991, 2012

chemical ozone destruction, and therefore to an increased ozone VMR (e.g. Finger et al., 1995). At altitudes below 10 hPa, increased cooling promotes more heterogeneous reactions. However, their efficiency also depends on water vapour concentrations as discussed by Shindell (2001). Model results analyzed here show that such anti-correlation can be seen down to altitudes corresponding to 30 hPa. Shepherd and Jonsson (2008) suggested that temperature variations should be considered in terms of changes in CO_2 and ODS, rather than ozone. They found that during 2010–2040, a period of rapid ODS decrease, up to 40 % of the increase in mean global upper stratospheric ozone (between 50–0.5 hPa) is attributed to CO_2 cooling, whereas during the depletion period of 1975–1995, only ~ 10 % of ozone loss is attributed to CO_2 cooling. This reflects the growing dominance of GHG concentrations during the ozone recovery period.

A decrease in temperature in the lower polar stratosphere, particularly within the polar vortex, results in an increase in the meridional temperature gradient at the vortex edge and thus enhances westerly zonal winds in this region. Circumpolar westerly zonal winds show an increase in magnitude during the period of ozone depletion with a corresponding decrease during ozone recovery for all months considered. Using a 15 $m s^{-1}$ minimum in zonal wind speed as a proxy for the polar vortex, the polar vortex was found to be present for all spring months across all altitudes considered, but broken up by December above 50 hPa. In the lowermost stratosphere, model simulations for December indicate a persisting vortex well into early summer, especially during the peak ozone depletion period around the year 2000. At pressures ≤ 70 hPa, the December vortex will last until approximately 2050, when December TOC returns to its 1975 baseline value. CCMVal-2 models indicate a response of zonal winds to recovering ozone, namely a decrease in wind speed with increasing ozone VMR. A wind response to changes in temperature, associated with ozone concentration, has about a one month time lag: maximal ozone gradients are seen in October–November, and maximum wind gradients are seen a month later, in November–December. Persistence of the polar vortex into the summer months could also be linked to a decreasing

ACPD
12, 18959–18991, 2012

planetary wave activity, which was described in (Monier and Weare, 2011). The breakdown of the polar westerlies is induced by dynamical heating from breaking planetary waves, and the timing of this breakdown in early summer can influence the propagation of gravity waves into the mesosphere, and thus potentially affecting the strength of the mesospheric branch of the Brewer-Dobson circulation (Smith et al., 2010).

In summary, based on median trends of CCMVal-2 REF-B2 model simulations, we conclude that due to combined effects of increasing GHG and decreasing halogen levels in the 21st century, Antarctic TOC will recover to 1975 baseline values in 2065–2075 in spring and in ~2050 in December. A delay in the vortex breakup, indicated by CCMVal-2 model median wind trends, leads to lower rates of TOC recovery in December. Anthropogenic ODS emissions dominate in the lowermost stratosphere, while CO_2 cooling dominates at higher altitudes. However, increase in GHG concentrations may start affecting ozone levels at the bottom of the stratosphere towards the end of the 21st century, when ODS no longer have a significant influence on atmospheric ozone over Antarctica. While numerous results related to regional and global ozone and climate applications have already been derived from CCMVal-2 model simulations (e.g. Eyring et al., 2010a), the present analysis focuses on unique aspects of future Antarctic ozone recovery that, according to our knowledge, have not been addressed before. Among various benefits for local and global climate change-related studies, results of this work, particularly rates of ozone recovery, are important for evaluating potential effects and impact of associated changes in surface UV radiation on the Antarctic climate and ecosystem.

In the future, model simulations with different GHG and ODS scenarios would help to attribute the magnitude of effects from anthropogenic forcings in predictions for TOC and ozone recovery. The provision of daily values for various metrics parameters used in this work, in conjunction with different assumptions on predicted anthropogenic forcings, would provide a more complete picture for the 21st century ozone recovery. For example, daily wind metrics, with a variety of future scenarios in the evolution of ODS and GHG concentrations, would enhance our ability to evaluate the extent of a delay

ACPD
12, 18959–18991, 2012

Title Page
Abstract | Introduction
Conclusions | References
Tables | Figures
◀ | ▶
◀ | ▶
Back | Close
Full Screen / Esc
Printer-friendly Version
Interactive Discussion

in the polar vortex breakup by considering the transition of westerly to easterly stratospheric polar winds and thus provide information beyond what is considered in Buchart et al. (2011). That study considers a single REF-B2 simulation during the observation period (1980–1999) and the date of when zonal-mean zonal wind speeds at 60° S becomes zero.

Acknowledgements. We acknowledge the modeling groups for making their simulations available for this analysis, the Chemistry-Climate Model Validation Activity (CCMVal) for the World Climate Research Programme's (WCRP) Stratospheric Processes and their Role in Climate (SPARC) project for organizing and coordinating the model data analysis activity, and the British Atmospheric Data Centre (BADC) for collecting and archiving the CCMVal model output. TOMS data are freely available from the NASA website http://acd-ext.gsfc.nasa.gov/Data_services/merged/. This work was sponsored in part by the Australian Antarctic Division Division under Australian Antarctic Science projects 737 and 2699. Part of this work was also supported by the Commonwealth Department of Environment, Water, Heritage and the Arts, grant 2008/02103.

References

Austin, J., Struthers, H., Scinocca, J., Plummer, D. A., Akiyoshi, H., Baumgaertner, A. J. G., Bekki, S., Bodeker, G. E., Braesicke, P., Brühl, C., Butchart, N., Chipperfield, M. P., Cugnet, D., Dameris, M., Dhomse, S., Frith, S., Garny, H., Gettelman, A., Hardiman, S. C., Jöckel, P., Kinnison, D., Kubin, A., Lamarque, J. F., Langematz, U., Mancini, E., Marchand, M., Michou, M., Morgenstern, O., Nakamura, T., Nielsen, J. E., Pitari, G., Pyle, J., Rozanov, E., Shepherd, T. G., Shibata, K., Smale, D., Teyssèdre, H., and Yamashita, Y.: Chemistry-climate model simulations of spring Antarctic ozone, J. Geophys. Res., 115, D00M11, doi:10.1029/2009JD013577, 2010.

Bais, A. F., Tourpali, K., Kazantzidis, A., Akiyoshi, H., Bekki, S., Braesicke, P., Chipperfield, M. P., Dameris, M., Eyring, V., Garny, H., Iachetti, D., Jöckel, P., Kubin, A., Langematz, U., Mancini, E., Michou, M., Morgenstern, O., Nakamura, T., Newman, P. A., Pitari, G., Plummer, D. A., Rozanov, E., Shepherd, T. G., Shibata, K., Tian, W., and Yamashita, Y.:

ACPD
12, 18959–18991, 2012

Future Antarctic ozone recovery rates

J. M. Siddaway et al.

Projections of UV radiation changes in the 21st century: impact of ozone recovery and cloud effects, Atmos. Chem. Phys., 11, 7533–7545, doi:10.5194/acp-11-7533-2011, 2011.
Buchart, N., Charlton-Perez, A. J., Cionni, I., Hardiman, S. C., Haynes, P. H., Krüger, K., Kushner, P. J., Newman, P. A., Osprey, S. M., Perlwitz, J., Sigmond, M., Wang, L., Akiyoshi, H., Austin, J., Bekki, S., Baumgaertner, A., Braesicke, P., Brühl, C., Chipperfield, M., Dameris, M., Dhomse, S., Eyring, V., Garcia, R., Garny, H., Jöckel, P., Lamarque, J. F., Marchand, M., Michou, M., Morgenstern, O., Nakamura, T., Pawson, S., Plummer, D., Pyle, J., Rozoanov, E., Scinocca, J., Shepherd, T. G., Shibata, K., Smale, D., Teyssèdre, H., Tian, W., Waugh, D., and Yamashita, Y.: Multimodel climate and variability of the stratosphere, J. Geophys. Res., 116, D05102, doi:10.1029/2010JD014995, 2011.
Dee, D. P., Uppala, S. M., Simmons, A. J., Berrisford, P., Poli, P., Kobayashi, S., Andrae, U., Balmaseda, M. A., Balsamo, G., Bauer, P., Bechtold, P., Beljaars, A. C. M., van de Berg, L., Bidlot, J., Bormann, N., Delsol, C., Dragani, R., Fuentes, M., Geer, A. J., Haimberger, L., Healy, S. B., Hersbach, H., Hólm, E. V., Isaksen, L., Kållberg, P., Köhler, M., Matricardi, M., McNally, A. P., Monge-Sanz, B. M., Morcrette, J. J., Park, B-K., Peubey, C., de Rosnay, P., Tavolato, C., Thépaut, J.-N., and Vitart, F.: The ERA-Interim reanalysis: configuration and performance of the data assimilation system, Q. J. Roy. Meteor. Soc., 137, 553–597, doi:10.1002/qj.828, 2011.
Deushi, M. and Shibata, K.: Impacts of increases in greenhouse gases and ozone recovery on lower stratospheric circulation and the age of air: chemistry-climate model simulations up to 2100, J. Geophys. Res., 116, D07107, doi:10.1029/2010JD015024, 2011.
Eyring, V., Waugh, D. W., Bodeker, G. E., Cordero, E., Akiyoshi, H., Austin, J., Beagley, S. R., Boville, B. A., Braesicke, P., Brühl, C., Buchart, N., Chipperfield, M. P., Dameris, M., Deckart, R., Deushi, M., Frith, S. M., Garcia, R. R., Gettelman, A., Giorgetta, M. A., Kinnison, D. E., Mancini, E., Manzini, E., Marsh, D. R., Matthes, S., Nagashima, T., Newman, P. A., Nielsen, J. E., Pawson, S., Pitari, G., Plummer, D. A., Rozanov, E., Schraner, M., Scinocca, J. F., Semeniuk, K., Shepherd, T. G., Shibata, K., Steil, B., Stolarski, R. S., Tian, W., and Yamashita, Y.: Multimodel projections of stratospheric ozone in the 21st century, J. Geophys. Res., 112, D16303, doi:10.1029/2006JD008332, 2007.
Eyring, V., Cionni, I., Bodeker, G. E., Charlton-Perez, A. J., Kinnison, D. E., Scinocca, J. F., Waugh, D. W., Akiyoshi, H., Bekki, S., Chipperfield, M. P., Dameris, M., Dhomse, S., Frith, S. M., Garny, H., Gettelman, A., Kubin, A., Langematz, U., Mancini, E., Marchand, M., Nakamura, T., Oman, L. D., Pawson, S., Pitari, G., Plummer, D. A., Rozanov, E.,

ACPD
12, 18959–18991, 2012

Shepherd, T. G., Shibata, K., Tian, W., Braesicke, P., Hardiman, S. C., Lamarque, J. F., Morgenstern, O., Pyle, J. A., Smale, D., and Yamashita, Y.: Multi-model assessment of stratospheric ozone return dates and ozone recovery in CCMVal-2 models, Atmos. Chem. Phys., 10, 9451–9472, doi:10.5194/acp-10-9451-2010, 2010a.

Eyring, V., Cionni, I., Lamarque, J. F., Akiyoshi, H., Bodeker, G. E., Charlton-Perez, A. J., Frith, S. M., Gettelman, A., Kinnison, D. E., Nakamura, T., Oman, L. D., Pawson, S., and Yamashita, Y.: Sensitivity of 21st century stratospheric ozone to greenhouse gas scenarios, Geophys. Res. Lett., 37, L16801, doi:10.1029/2010GL044443, 2010b.

Farman, J. C., Gardner, B. G., and Shanklin, J. D.: Large losses of total ozone in Antarctica reveal seasonal ClO_x/NO_x interaction, Nature, 315, 207–210, 1985.

Finger, F. G., Nagatani, R. M., Gelman, M. E., Long, C. S., and Miller, A. J.: Consistency between variations of ozone and temperature in the stratosphere, Geophys. Res. Lett., 22, 3477–3480, 1995.

Grytsai A. V., Evtushevsky, O. M., Agapitov, O. V., Klekociuk, A. R., and Milinevsky, G. P.: Structure and long-term change in the zonal asymmetry in Antarctic total ozone during spring, Ann. Geophys., 25, 361–374, 2007, http://www.ann-geophys.net/25/361/2007/.

Hassler, B., Daniel, J. S., Johnson, B. J., Solomon, S., and Oltmans, S. J.: An assessment of changing ozone loss rates at South Pole: twenty-five years of ozonesonde measurements, J. Geophys. Res., 116, D22301, doi:10.1029/2011JD016353, 2011.

IPCC (Intergovernmental Panel on Climate Change): Special Report on Emissions Scenarios: a Special Report Of Working Group III of the Intergovernmental Panel on Climate Change, Cambridge University Press, Cambridge, UK, 599 pp., 2000.

Klekociuk, A. R., Tully, M. B., Alexander, S. P., Dargaville, R. J., Deschamps, L. L., Fraser, P. J., Gies, H. P., Henderson, S. I., Javorniczky, J., Krummel, P. B., Petelina, S. V., Shanklin, J. D., Siddaway, J. M., and Stone, K. A.: The Antarctic ozone hole during 2010, Aust. Meteorol. Ocean. J., 61, 253–267, 2011.

Lee, A. M., Roscoe, H. K., Jones, A. E., Haynes, P. H., Schuckburgh, E. F., Morrey, M. W., and Pumphrey, H. C.: The impact of the mixing properties within the Antarctic stratospheric vortex on ozone loss in spring, J. Geophys. Res., 106, 3203–3211, 2001.

Monier, E. and Weare, B. C.: Climatology and trends in the forcing of the stratospheric zonal-mean flow, Atmos. Chem. Phys., 11, 12751–12771, doi:10.5194/acp-11-12751-2011, 2011.

ACPD
12, 18959–18991, 2012

Future Antarctic ozone recovery rates

J. M. Siddaway et al.

Morgenstern, O., Giorgetta, M. A., Shibata, K., Eyring, V., Waugh, D. W., Shepherd, T. G., Akiyoshi, H., Austin, J., Baumgaertner, A. J. G., Bekki, S., Braesicke, P., Brühl, C., Chipperfield, M. P., Cugnet, D., Dameris, M., Dhomse, S., Frith, S. M., Garny, H., Gettelman, A., Hardiman, S. C., Hegglin, M. I., Jöckel, P., Kinnison, D. E., Lamarque, J.-F., Mancini, E., Manzini, E., Marchand, M., Michou, M., Nakamura, T., Nielsen, J. E., Olivié, D., Pitari, G., Plummer, D. A., Rozanov, E., Scinocca, J. F., Smale, D., Teyssèdre, H., Toohey, M., Tian, W., and Yamashita, Y.: Review of the formulation of present-generation stratospheric chemistry-climate models and associated external forcings, J. Geophys. Res., 115, D00M02, doi:10.1029/2009JD013728, 2010.

Nash, E. R., Newman, P. A., Rosenfield, J. E., and Schoeber, M. R.: An objective determination of the polar vortex usig Ertel's potential vorticity, J. Geophys. Res., 101, 9471–9478, 1996.

Newman, P. A., Kawa, S. R., and Nash, E. R.: On the size of the Antarctic ozone hole, Geophys. Res. Lett., 31, L21104, doi:10.1029/2004GL020596, 2004.

Newman, P. A., Nash, E. R., Kawa, S. R., Montzka, S. A., and Schauffler, S. M.: When will the Antarctic ozone hole recover?, Geophys. Res. Lett., 33, L12814, doi:10.1029/2005GL025232, 2006.

Newman, P. A., Daniel, J. S., Waugh, D. W., and Nash, E. R.: A new formulation of equivalent effective stratospheric chlorine (EESC), Atmos. Chem. Phys., 7, 4537–4552, doi:10.5194/acp-7-4537-2007, 2007.

Perlwitz, J., Pawson, S., Fogt, R. L., Nielsen, J. E., and Neff, W. D.: Impact of stratospheric ozone recovery on Antarctic climate, Geophys. Res. Lett., 35, L08714, doi:10.1029/2008GL033317, 2008.

Randel, W. J., Shine, K. P., Austin, J., Barnett, J., Claud, C., Gillett, N. P., Keckhut, P., Langematz, U., Lin, R., Long, C., Mears, C., Miller, A., Nash, J., Seidel, D. J., Thompson, D. W. J., Wu, F., and Yoden, S.: An update of observed stratospheric trends, J. Geophys. Res., 114, D02107, doi:10.1029/2008JD010421, 2009.

Salby, M., Titova, E., and Deschamps, L.: Rebound of Antarctic ozone, Geophys. Res. Lett., 38, L09702, doi:10.1029/2011GL047266, 2011.

Shepherd, T. G. and Jonsson, A. I.: On the attribution of stratospheric ozone and temperature changes to changes in ozone-depleting substances and well-mixed greenhouse gases, Atmos. Chem. Phys., 8, 1435–1444, doi:10.5194/acp-8-1435-2008, 2008.

Smith, A. K., Garcia, R. R., Marsh, D. R., Kinnison, D. E., and Richter, J. H.: Simulations of the response of mesospheric circulation and temperature to the Antarctic ozone hole, Geophys. Res. Lett., 37, L22803, doi:10.1029/2010GL045255, 2010.

Shindell, D. T.: Climate and ozone response to increased stratospheric water vapor, Geophys. Res. Lett., 28, 1551–1554, doi:10.1029/1999GL011197, 2001.

Shindell, D. T. and Schimdt, G. A.: Southern Hemisphere climate response to ozone changes and greenhouse gas increases, Geophys. Res. Lett., 31, L18209, doi:10.1029/2004GL020724, 2004.

Solomon, S.: Stratospheric ozone depletion: a review of concepts and history, Rev. Geophys., 37, 275–316, 1999.

Solomon, S., Garcia, R. R., Rowland, F. S., and Wuebbles, D. J.: On the depletion of Antarctic ozone, Nature, 321, 895–899, 1986.

Solomon, S., Portmann, R. W., Sasaki, T., Hofmann, D. J., and Thompson, D. W. J.: Four decades of ozonesonde measurements over Antarctica, J. Geophys. Res., 110, D21311, doi:10.1029/2005JD005917, 2005.

Son, S. W., Gerber, E. P., Perlwitz, J., Polvani, L. M., Gillett, N. P., Seo, K. H., Eyring, V., Shepherd, T. G., Waugh, D., Akiyoshi, H., Austin, J., Baumgaerter, A., Bekki, S., Braesicke, P., Brühl, C., Buchart, N., Chipperfield, M. P., Cugnet, D., Dameris, M., Dhomse, S., Frith, S. M., Garny, H., Garcia, R., Hardiman, S. C., Jöckel, P., Lamarque, J. F., Mancini, E., Marchand, M., Michou, M., Nakamura, T., Morgenstern, O., Pitari, G., Plummer, D. A., Pyle, J., Rozanov, E., Scinocca, J. F., Shibata, K., Smale, D., Teyssèdre, H., Tian, W., and Yamashita, Y.: Impact of stratospheric ozone on Southern Hemisphere circulation change: a multimodel assessment, J. Geophys. Res., 115, D00M07, doi:10.1029/2010JD014271, 2010.

SPARC CCMVal: SPARC Report on the Evaluation of Chemistry-Climate Models, SPARC Rep. 5, edited by: Eyring, V., Shepherd, T. G., and Waugh, D. W., World Clim. Res. Programme, available at: http://www.atmosp.physics.utoronto.ca/SPARC, 2010.

Stolarski, R. S. and Frith, S. M.: Search for evidence of trend slow-down in the long-term TOMS/SBUV total ozone data record: the importance of instrument drift uncertainty, Atmos. Chem. Phys., 6, 4057–4065, doi:10.5194/acp-6-4057-2006, 2006.

Thompson, D. W. J. and Solomon, S.: Interpretation of recent Southern Hemisphere climate change, Science, 296, 895–899, 2002.

Waugh, D. W., Randel, W. J., Pawson, S., Newman, P. A., and Nash, E. R.: Persistence of the lower stratospheric polar vortices, J. Geophys. Res., 104, 27191–27201, 1999.

Waugh, D. W., Oman, L., Kawa, S. R., Stolarski, R. S., Pawson, S., Douglass, A. R., Newman, P. A., and Nielsen, J. E.: Impacts of climate change on stratospheric ozone recovery, Geophys. Res. Lett., 36, L03805, doi:10.1029/2008GL036223, 2009.

Waugh, D. W. and Polvani, L. M.: Stratospheric polar vortices, in: The Stratosphere: Dynamics, Transport, and Chemistry, edited by: Polvani, L. M., Sobel, A. H., and Waugh, D. W., Geophysical Monograph Series, Vol. 190, doi:10.1029/2009GM000887, 2010.

Wirth, V.: Quasi-stationary planetary waves in total ozone and their correlation with lower stratospheric temperature, J. Geophys. Res., 98, 8873–8882, 1993.

World Meteorological Organization (WMO): Scientific Assessment of Ozone Depletion: 2006, Rep. 50, Global Ozone Research and Monitoring Project, World Meterol. Organ., Geneva, Switzerland, 2007.

Zeng, G., Morgenstern, O., Braesicke, P., and Pyle, J. A.: Impact of stratospheric ozone recovery on tropospheric ozone and its budget, Geophys. Res. Lett., 37, L09805, doi:10.1029/2010GL042812, 2010.

ACPD
12, 18959–18991, 2012

Table 1. Decadal TOC recovery rate poleward of 60° S as a percentage of the 1975 baseline value. Italicized numbers indicate decades when TOC has exceeded its baseline value.

Year	00–09	10–19	20–29	30–39	40–49	50–59	60–69	70–79	80–89
Sep	2.01	3.92	5.30	5.71	3.85	2.78	1.96	*2.45*	*0.91*
Oct	2.6	3.61	6.13	5.96	5.12	5.06	*1.34*	*1.96*	*1.6*
Nov	1.05	2.57	4.99	4.51	4.51	4.41	*2.23*	*1.37*	*0.45*
Dec	0.59	0.41	4.31	2.09	3.17	*4.11*	*0.1*	*1.08*	*1.32*

ACPD
12, 18959–18991, 2012
Future Antarctic ozone recovery rates
J. M. Siddaway et al.

Table 2. Decadal TOC recovery rate (DU decade^{-1}) poleward of 60° S. Italicized numbers indicate decades when TOC has exceeded its 1975 baseline value.

Year	00–09	10–19	20–29	30–39	40–49	50–59	60–69	70–79	80–89
Sep	6.01	11.75	15.84	17.07	11.51	8.31	5.86	*7.32*	*2.73*
Oct	7.86	10.94	18.54	18.01	15.48	15.29	*4.07*	*5.91*	*4.83*
Nov	3.44	8.46	16.43	14.83	14.84	14.50	*7.32*	*4.52*	*1.48*
Dec	2.06	1.44	15.07	7.30	11.08	*14.36*	*0.31*	*3.76*	*4.62*

ACPD
12, 18959–18991, 2012

Future Antarctic ozone recovery rates

J. M. Siddaway et al.

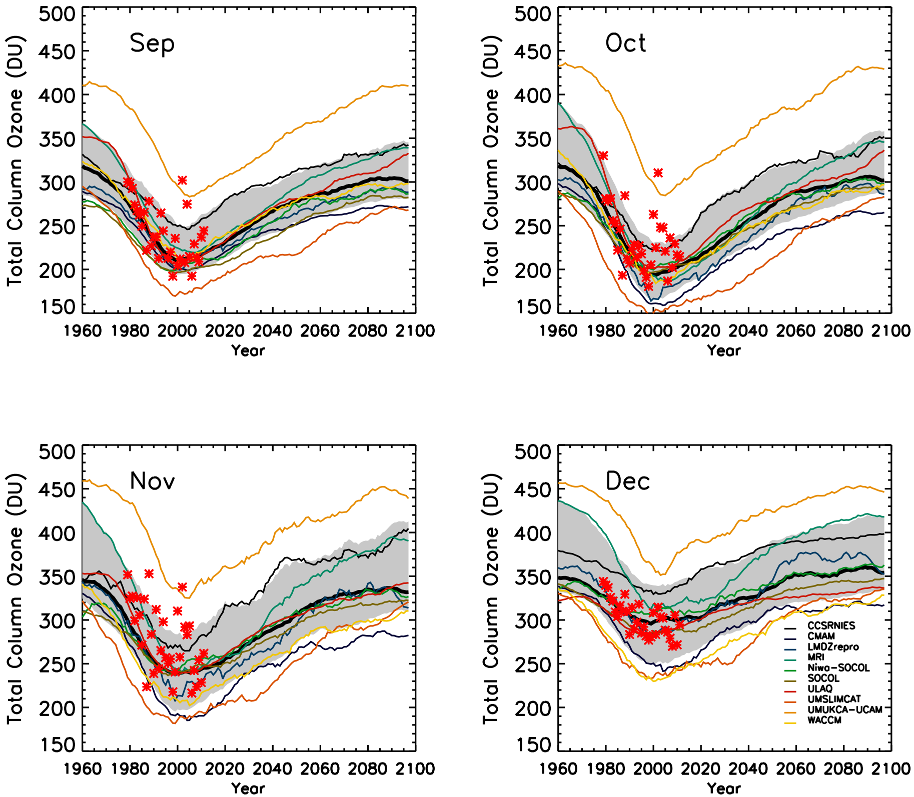

Fig. 1. Monthly total column ozone (TOC) time series zonally averaged poleward of 60° S from selected REF-B2 model simulations. Thick black line is the multi-model median, grey area represents the 95 % confidence limit of the median derived using a bootstrapping method. Red stars indicate TOC zonally averaged monthly values poleward of 62.5° S from the TOMS version 8.5 merged ozone dataset (MOD) for 1979–2011.

ACPD
12, 18959–18991, 2012

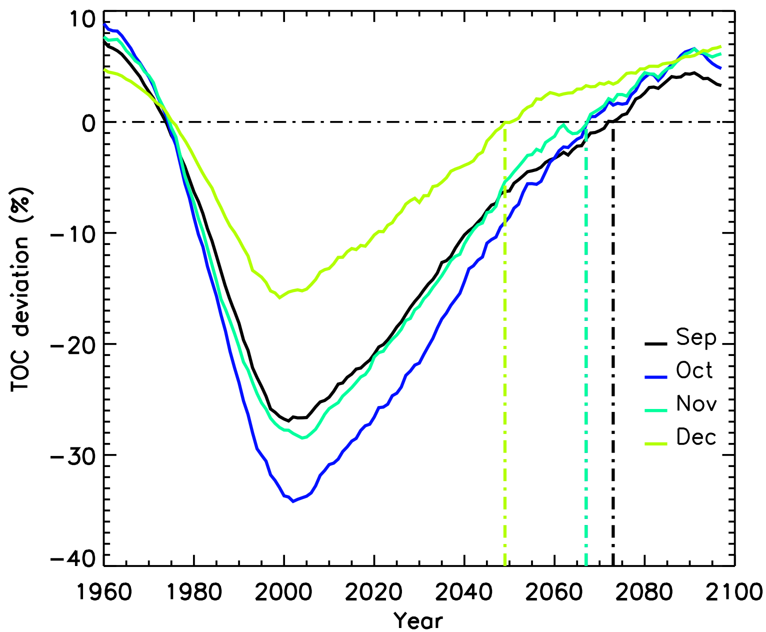

Fig. 2. Time series of multi-model TOC median values for September–December as percent deviations from the 1975 baseline. TOC return dates are shown by dashed-dotted lines color-coded by the corresponding month.

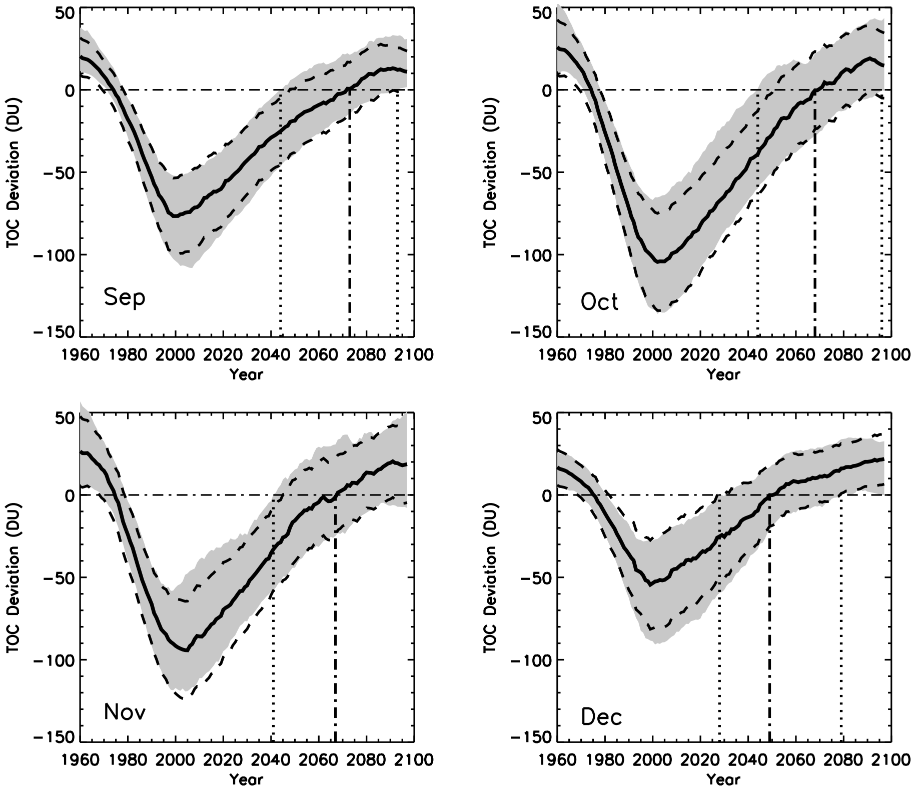

Fig. 3. Time series of deviations for multi-model median TOC from the 1975 baseline for each month. Median TOC return dates are shown by the vertical dot-dashed lines, shaded area is the 95 % confidence limit of the median, dashed curves show the median absolute deviation range with corresponding upper and lower limits range of return dates shown by vertical dotted lines.

ACPD
12, 18959–18991, 2012

Future Antarctic ozone recovery rates

J. M. Siddaway et al.

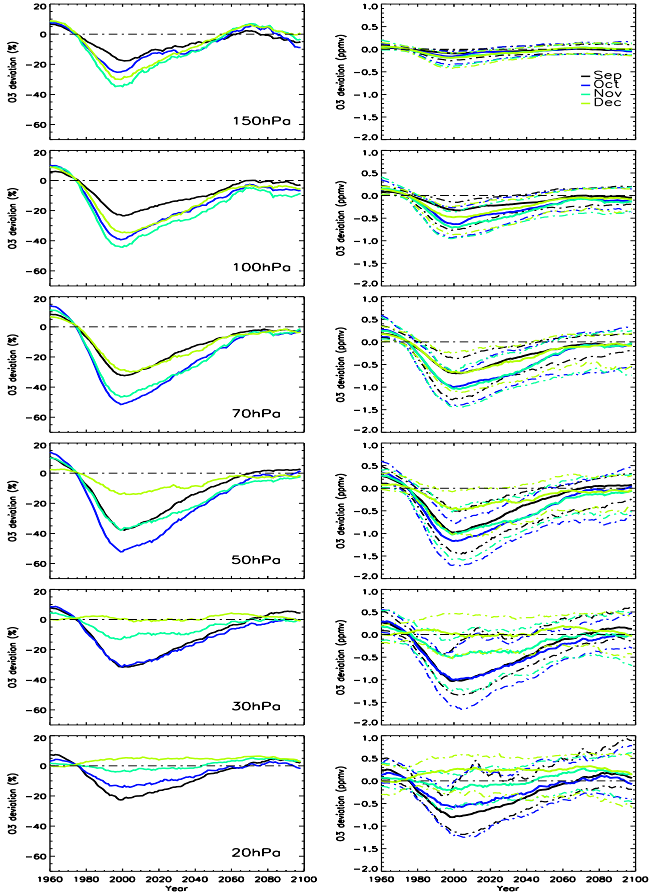

Fig. 4. Deviations of monthly multi-model median ozone VMR from 1975 baseline, zonally averaged poleward of 60° S for selected pressure levels from 150 hPa to 20 hPa. Left panels – percent deviations, right panels – absolute deviations. Dashed lines indicate 95 % confidence level of median.

ACPD
12, 18959–18991, 2012

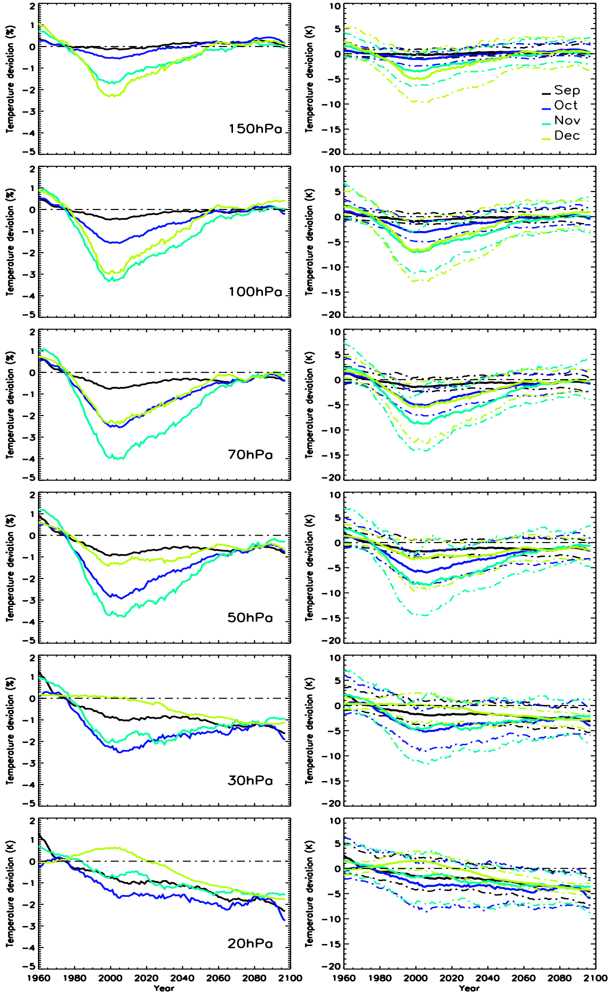

Fig. 5. Same as in Fig. 4, but for multi-model median temperatures.

Discussion Paper | Discussion Paper | Discussion Paper | Discussion Paper

ACPD

12, 18959–18991, 2012

Future Antarctic ozone recovery rates

J. M. Siddaway et al.

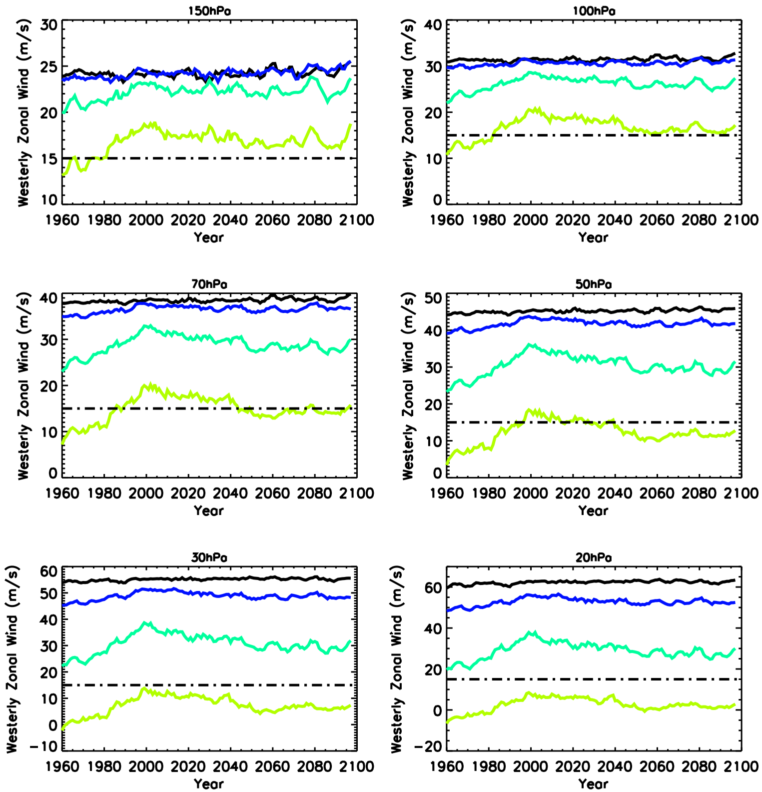

Fig. 6. Time series of monthly zonal mean zonal wind speed averaged across 50°–70° S at 150–20 hPa. Dot-dashed lines indicate the minimum wind velocity of 15 m s^{-1} that identifies the polar vortex edge. Colors correspond to same months as in Fig. 4.

ACPD
12, 18959–18991, 2012

Future Antarctic ozone recovery rates

J. M. Siddaway et al.

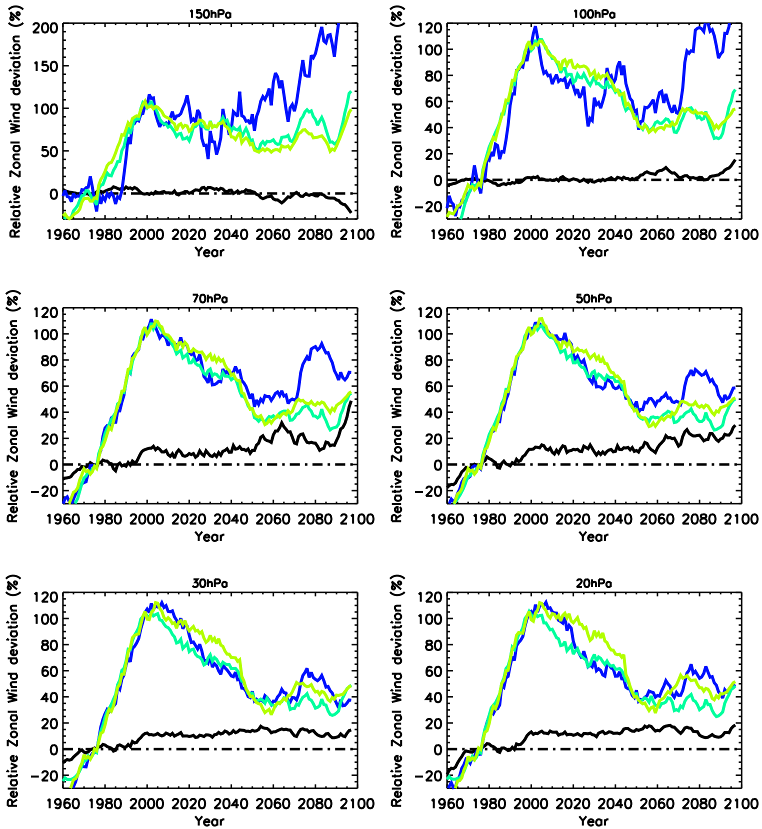

Fig. 7. Normalized time series of percent deviation of zonal mean zonal wind speed averaged over 50°–70° S. For full description see text. The September wind data have been scaled – divided by 100 for 150 and 100 hPa, and divided by 10 everywhere else. Colors correspond to same months as in Fig. 4.

ACPD
12, 18959–18991, 2012

Future Antarctic ozone recovery rates

J. M. Siddaway et al.